
ARTICLE

Evaluation of Solute-Atom Clusters Segregated in α -Fe

Chikashi SUZUKI*, Tomohito TSURU and Yoshiyuki KAJI

*Nuclear Science and Engineering Directorate, Japan Atomic Energy Agency,
2-4 Shirakata Shirane, Tokai-mura, Naka-gun, Ibaraki-ken, 319-1195, Japan*

We examined the interaction between impurities in α -Fe such as Cu, Si, and Ni, using the density functional theory (DFT) calculation. This examination indicated that the bond of Cu-Si was more stable than that of Si-Si, and that the interaction parameters of Cu-Si and Si-Ni were lower than that of Si-Si. This indicated that Cu and Ni impurities encouraged segregation of solute-atom clusters containing Si atoms but that the interaction of Cu-Ni was small. In addition, we evaluated the effect of the coexistence of impurities in the view point of the electronic structure. The electronic structure showed that the coexistence of Cu and Si lowered energy of Cu and adjacent Fe component. This suggested that the coexistence of Cu and Si stabilized Cu and adjacent Fe component.

KEYWORDS: *segregation, impurity, solute-atom cluster, interaction parameter, electronic structure*

I. Introduction

It has been important to obtain the understanding of the controlling mechanism that causes reactor pressure vessel (RPV) embrittlement. This involves detailed characterization of the irradiation-induced microstructural changes and their dependence on material and irradiation parameter. Especially it is noted that the segregation and clustering are observed as the form of solute-atom clusters in low alloy steels of RPV irradiated for many years. These clusters are thought to be the causes of irradiation-induced embrittlement.¹⁻⁵⁾ Among impurities of low alloy steels of RPV, Cu has been thought to be dominant constituent for solute-atom clusters. In recent years, the three-dimensional atom probe (3DAP) observation of the surveillance test specimens of irradiated low alloy steels of RPV indicates that clusters segregated in these specimens contain other elements than Cu such as Ni, Mn, Si, and P.⁶⁾ Besides, solute-atom clusters are observed in the specimens of low-Cu alloy steels of RPV and Cu is not dominant constituent in these clusters.⁷⁾ Furthermore, the 3DAP observation of irradiated ferrite model alloys shows that the component fractions of Ni, Mn, and Si in solute-atom clusters are similar and much larger than those of the ferrite model alloys for various values of Cu concentration and cluster size.^{8,9)}

Tsuru *et al.*¹⁰⁾ investigated the impurity segregation in α -Fe using the density functional theory (DFT) calculation in detail, and predicted this segregation for various impurity elements. However, a few elements are observed as the form of solute-atom clusters though it is predicted that the cluster creation is unstable. Besides, Ohmura *et al.*¹¹⁾ evaluated the interaction between impurity atoms and vacancies in detail.

In this study, in order to examine the behaviors of some elements such as Cu, Si, and Ni of the high concentration for

the solute-atom clusters as a fundamental investigation, we perform the DFT calculation for these clusters, because the short-range interaction between first or second neighboring atoms in solute-atom clusters of nano-size and the interaction between different elements are likely to be important. Moreover, we evaluate these interactions from the view point of the electronic structure.

II. Calculation

In this study, we used the DFT calculation code PHASE ver. 7.01¹²⁾ with a periodic boundary condition. Exchange-correlation energy was described using the Perdew-Burke-Ernzerhof (PBE) gradient-corrected exchange-correlation function within the generalized gradient approximation (GGA),¹³⁾ with spin polarization. The core electrons of all atoms were treated via ultra-soft pseudo potentials^{14,15)} with a cut-off of 500 eV. The geometry optimization was performed using a $7 \times 7 \times 7$ Monkhorst-Pack k-point mesh. A Fermi smearing of 0.2 eV was utilized and the corrected energy was extrapolated to zero Kelvin.

The average composition values of Si and Ni in the solute-atom cluster in irradiated ferrite model alloys show high-concentration of 3-20%, though those before the irradiation are below 2.0%.^{8,9)} The average composition value of Cu in the solute-atom cluster is much larger than those before the irradiation.^{8,9)} For simplicity for various composition values, crystal structure of α -Fe is bcc and the calculations were performed on $2 \times 2 \times 2$ supercells (16 atoms), which are Fe_{16} , CuFe_{15} , SiFe_{15} , and NiFe_{15} . The short-range interactions between first or second neighboring atoms are likely to be significant due to the nano-size of the solute-atom cluster in addition to the high concentration of impurities, so that the models of $\text{Cu}_2\text{Fe}_{14}$, $\text{Si}_2\text{Fe}_{14}$, $\text{Ni}_2\text{Fe}_{14}$, CuSiFe_{14} , CuNiFe_{14} , and SiNiFe_{14} are calculated for two kinds considering the first and second neighboring bonds between impurities (Cu,

*Corresponding author, E-mail: suzuki.chikashi@jaea.go.jp

Si, and Ni). The calculated lattice constant of supercell is 5.69 Å, which is comparable to the value in the literature.¹⁶⁾ Geometry optimizations were stopped when all the forces were smaller than 0.02 eV/Å. No symmetry constraints are imposed. For simplicity, the effect of stress relaxation is not taken in account.

III. Result and Discussion

1. Interaction between Impurities

We examine the interaction between impurities such as Cu, Ni, and Si atoms for the fundamental investigation. These elements are observed in the irradiated α -Fe metal. The first neighboring interaction between impurities is defined as.

$$\begin{aligned} E_{\text{int}}^{1\text{st}}(I_a - I_b) \\ = E^{1\text{st}}(I_a I_b \text{Fe}_{14}) + E(\text{Fe}_{16}) - E(I_a \text{Fe}_{15}) - E(I_b \text{Fe}_{15}) \quad (1) \end{aligned}$$

Here, I_a and I_b are expressed as impurity elements, and $E^{1\text{st}}$ ($I_a I_b \text{Fe}_{14}$), $E(\text{Fe}_{16})$, $E(I_a \text{Fe}_{15})$, and $E(I_b \text{Fe}_{15})$ are energy values of $I_a I_b \text{Fe}_{14}$ (first neighboring bond of $I_a - I_b$), Fe_{16} , $I_a \text{Fe}_{15}$, and $I_b \text{Fe}_{15}$ in the unit cell. The second neighboring interaction between impurities is also defined as,

$$\begin{aligned} E_{\text{int}}^{2\text{nd}}(I_a - I_b) \\ = E^{2\text{nd}}(I_a I_b \text{Fe}_{14}) + E(\text{Fe}_{16}) - E(I_a \text{Fe}_{15}) - E(I_b \text{Fe}_{15}) \quad (2) \end{aligned}$$

We consider this interaction between first neighboring atoms and that between second neighboring atoms, because that between second neighboring atoms cannot be ignored in bcc metals. The interactions between impurities are shown in **Table 1**.

Table 1 shows that the stability of the interaction between impurities is Cu-Cu > Ni-Ni > Si-Si. This tendency is coincident with the calculation¹⁰⁾ with larger unit cell of 54 atoms. The first neighboring interaction of Cu-Cu and Ni-Ni is more strong than second neighboring one in this calculation, because the absolute values of the first neighboring interaction is larger than those of the second neighboring. Compared with Cu-Cu and Ni-Ni bond, the second neighboring interaction is important for Si-Si bond, because the absolute value of the second neighboring interaction is comparable to that of the first neighboring.

Table 1 Interaction between impurities in α -Fe

Unit cell	Impurity co-ordination	Interaction (eV)
$\text{Cu}_2\text{Fe}_{14}$	First neighboring	-0.19
$\text{Cu}_2\text{Fe}_{14}$	Second neighboring	-0.11
$\text{Si}_2\text{Fe}_{14}$	First neighboring	0.41
$\text{Si}_2\text{Fe}_{14}$	Second neighboring	0.47
$\text{Ni}_2\text{Fe}_{14}$	First neighboring	0.21
$\text{Ni}_2\text{Fe}_{14}$	Second neighboring	0.11
CuSiFe_{14}	First neighboring	-0.04
CuSiFe_{14}	Second neighboring	0.06
CuNiFe_{14}	First neighboring	0.01
CuNiFe_{14}	Second neighboring	0.02
SiNiFe_{14}	First neighboring	0.12
SiNiFe_{14}	Second neighboring	0.35

We examine the interaction between different impurities. This examination shows that the bond between Cu and Si is more stable than that between Si atoms. This interaction indicates that Cu impurity encourages segregation of solute-atom clusters containing Si. On the other hand, the first neighboring bond of Si-Ni is more stable than those of Ni-Ni and of Si-Si.

This stability of the bonds of Cu-Si reflects the observation of the segregation of the solute-atom cluster containing both Cu and Si,^{6,8,9)} though the Si cluster is likely to be unstable in the analysis considering the bonds of Si-Si and Si-Fe causing the creation of Si clusters in α -Fe.¹⁰⁾

In these calculations, there is one first neighboring bond between impurities and there are two second ones. In the regular solution approximation, the first neighboring interaction between impurities is expressed as

$$\begin{aligned} E_{\text{int}}^{1\text{st}}(I_a - I_b) &= e_{I_a - I_b}^{1\text{st}} + e_{\text{Fe-Fe}}^{1\text{st}} - e_{I_a - \text{Fe}}^{1\text{st}} - e_{I_b - \text{Fe}}^{1\text{st}} \\ &= \frac{\Omega_{I_a - I_b}^{1\text{st}}}{8N} + \frac{1}{2} E_{\text{int}}^{1\text{st}}(I_a - I_a) + \frac{1}{2} E_{\text{int}}^{1\text{st}}(I_b - I_b) \quad (3) \end{aligned}$$

Here, $e_{I_a - I_b}^{1\text{st}}$, $e_{\text{Fe-Fe}}^{1\text{st}}$, $e_{I_a - \text{Fe}}^{1\text{st}}$, and $e_{I_b - \text{Fe}}^{1\text{st}}$ are first neighboring bond energy values of $I_a - I_b$, Fe-Fe, $I_a - \text{Fe}$, and $I_b - \text{Fe}$, and N is the numbers of atoms. The second neighboring interaction between impurities is also expressed as

$$\begin{aligned} E_{\text{int}}^{2\text{nd}}(I_a - I_b) &= e_{I_a - I_b}^{2\text{nd}} + e_{\text{Fe-Fe}}^{2\text{nd}} - e_{I_a - \text{Fe}}^{2\text{nd}} - e_{I_b - \text{Fe}}^{2\text{nd}} \\ &= \frac{\Omega_{I_a - I_b}^{2\text{nd}}}{3N} + \frac{1}{2} E_{\text{int}}^{2\text{nd}}(I_a - I_a) + \frac{1}{2} E_{\text{int}}^{2\text{nd}}(I_b - I_b) \quad (4) \end{aligned}$$

The interaction parameter between impurities per atom considering the first and second neighboring bond energy is expressed as

$$\begin{aligned} \frac{\Omega_{I_a - I_b}}{N} &= \frac{\Omega_{I_a - I_b}^{1\text{st}}}{N} + \frac{\Omega_{I_a - I_b}^{2\text{nd}}}{N} \\ &= 8E_{\text{int}}^{1\text{st}}(I_a - I_b) - 4E_{\text{int}}^{1\text{st}}(I_a - I_a) - 4E_{\text{int}}^{1\text{st}}(I_b - I_b) \\ &\quad + 3E_{\text{int}}^{2\text{nd}}(I_a - I_b) - \frac{3}{2} E_{\text{int}}^{2\text{nd}}(I_a - I_a) - \frac{3}{2} E_{\text{int}}^{2\text{nd}}(I_b - I_b) \quad (5) \end{aligned}$$

Table 2 shows the interaction parameter between impurities per atom. These indicate that the bonds of Cu-Si are more stable than the separately created bonds of Si-Si and Cu-Cu as described above. It is noted that the bonds of Si-Ni are also more stable. On the other hand, the stability of the bonds of Cu-Ni is comparable to that of the separately created bonds of Ni-Ni and Cu-Cu. This suggests that the segregation of the solute-atom cluster containing Si with Cu and Ni is likely to be encouraged, but that the interaction between Cu and Ni is small.

Table 2 Interaction parameter between impurities

Impurities	Interaction parameter (eV)
Cu and Si	-1.57
Cu and Ni	0.07
Si and Ni	-1.34

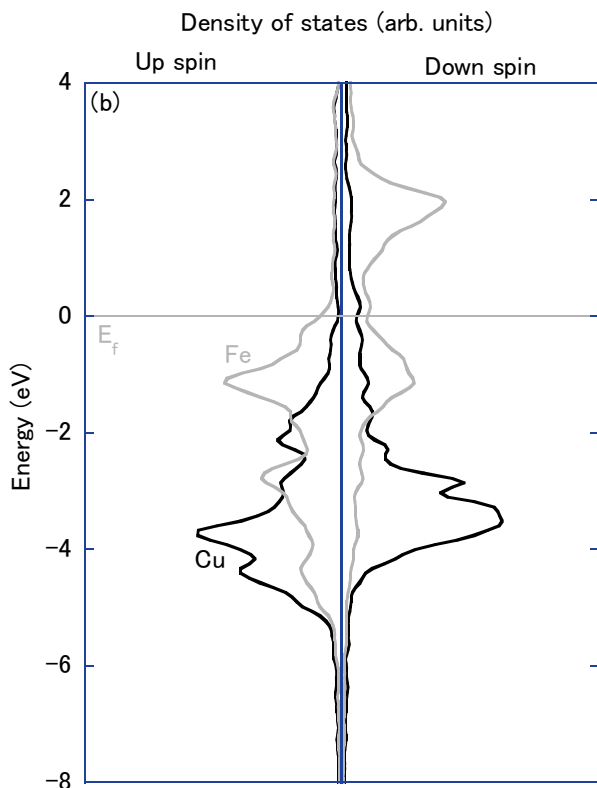
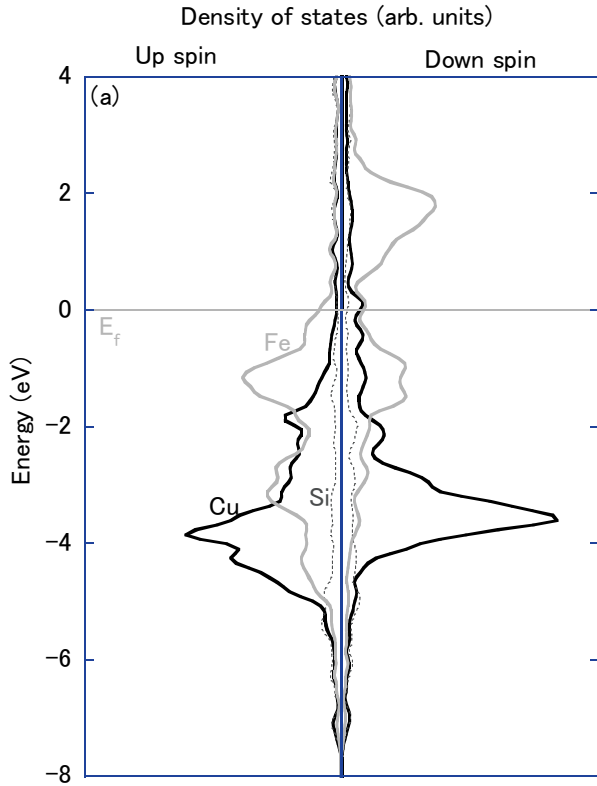


Fig. 1 (a) Density of states (DOS) of Cu and adjacent Fe of Cu-SiFe₁₄ and (b) that of Cu₂Fe₁₄, whose bonds of Cu-Si and Cu-Cu are first neighboring.

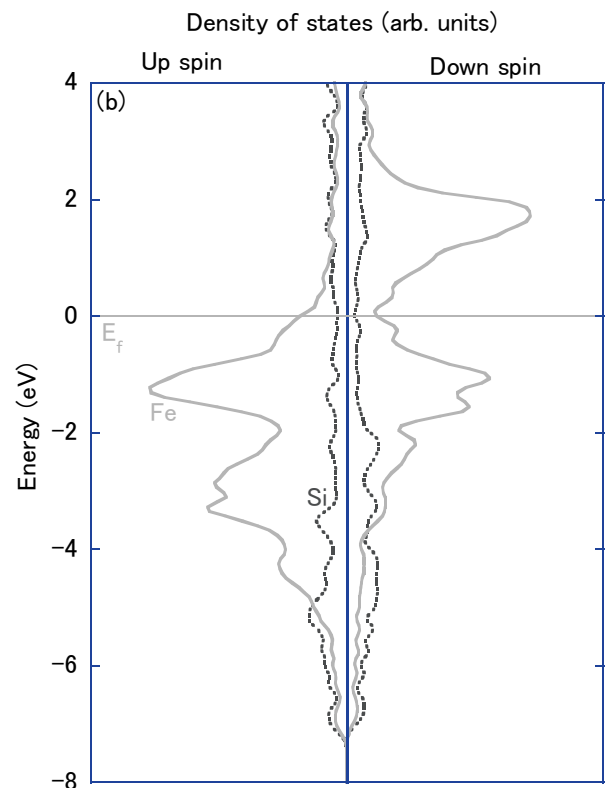
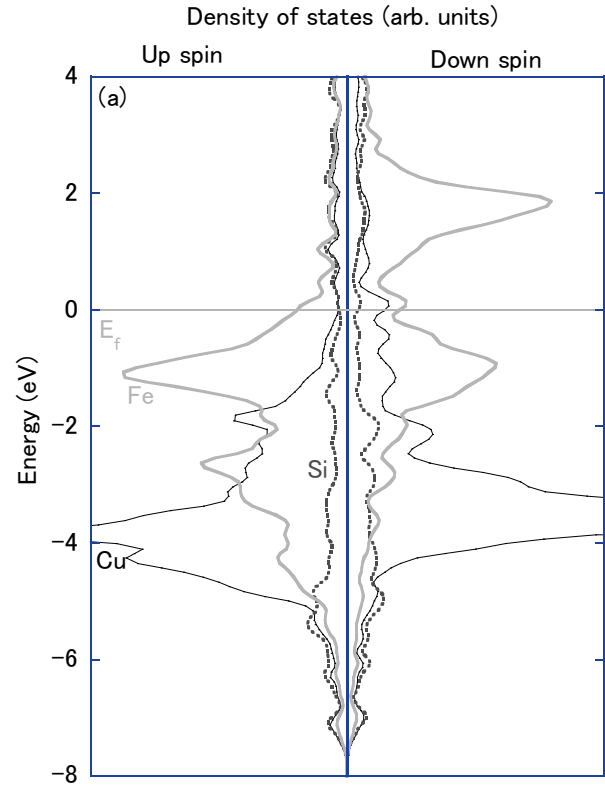


Fig. 2 (a) Density of states (DOS) of Si and adjacent Fe of Cu-SiFe₁₄ and (b) that of Si₂Fe₁₄, whose bonds of Cu-Si and Si-Si are first neighboring.

2. Electronic Structure of Fe, Cu, and Si

Tables 1 and 2 show that coexistence of Cu and Si is stable. In order to evaluate the effect of the coexistence of Cu and Si, **Figure 1** shows (a) density of states (DOS) of Cu and adjacent Fe of CuSiFe_{14} and (b) that of $\text{Cu}_2\text{Fe}_{14}$, whose bonds of Cu-Si and Cu-Cu are first neighboring.

These figures indicate that up spin DOS of Cu of CuSiFe_{14} in the occupied range has a peak at -3.9 eV and that that of $\text{Cu}_2\text{Fe}_{14}$ has a peak at -3.8 eV. It is noted that down spin DOS of Cu of CuSiFe_{14} in the occupied range has a peak at -3.6 eV, but that of $\text{Cu}_2\text{Fe}_{14}$ has a smaller peaks at -3.5 eV and -2.9 eV. These electronic structures of Cu suggest that Cu component is of lower energy in CuSiFe_{14} than in $\text{Cu}_2\text{Fe}_{14}$. On the other hand, DOS of Fe adjacent to Cu of CuSiFe_{14} is of a little lower energy than that of $\text{Cu}_2\text{Fe}_{14}$.

Figure 2 shows (a) density of states (DOS) of Si and adjacent Fe of CuSiFe_{14} and (b) that of $\text{Si}_2\text{Fe}_{14}$, whose bonds of Cu-Si and Si-Si are first neighboring. DOS's of Si and adjacent Fe of CuSiFe_{14} are similar to those of $\text{Si}_2\text{Fe}_{14}$. These electronic structures shown in Figs. 1 and 2 suggest that the coexistence of Cu and Si stabilizes Cu and adjacent Fe component.

The electronic structures of Si, Ni, and Fe adjacent to Ni of SiNiFe_{14} , whose bond of Si-Ni is first neighboring, are different from those of $\text{Si}_2\text{Fe}_{14}$ and $\text{Ni}_2\text{Fe}_{14}$. These differences are likely to cause the energy stabilization of SiNiFe_{14} .

The electronic structures of Cu, Ni, and Fe adjacent to Ni of CuNiFe_{14} , whose bond of CuNi is first neighboring, are similar to those of $\text{Cu}_2\text{Fe}_{14}$ and $\text{Ni}_2\text{Fe}_{14}$. This similarity suggests that the interaction parameter of Cu-Ni is small. Consequently, the effect of the coexistence of Cu and Ni is small.

IV. Conclusion

We calculated the electronic state of α -Fe containing Cu, Si, and Ni to examine the interaction between these impurities. This calculation indicated that the stability of the interaction between impurities was Cu-Cu > Ni-Ni > Si-Si, and that the bonds of Cu-Si and Si-Ni were more stable than that of Si-Si. In addition, we estimated the interaction parameter between impurities considering first and second neighboring interaction. This estimation suggested that the interaction parameters of Cu-Si and Si-Ni were stable and that Cu and Ni impurity encouraged segregation of solute-atom clusters containing Si atoms.

We evaluated the effect of the coexistence of impurities from the view point of the electronic structure. In case of coexistence of Cu and Si, the energy of Cu and adjacent Fe component was lowered. This electronic structure suggested that the coexistence of Cu and Si stabilized Cu and adjacent Fe component. As for the coexistence of Si and Ni, the difference of the electronic structures was likely to cause the energy stabilization. On the other hand, the effect of the coexistence of Cu and Ni was small.

References

- 1) G. R. Odette, "On the dominant mechanism of irradiation embrittlement of reactor pressure vessel steels," *Scripta Metall.*, **17**[10], 1183-1186 (1983).
- 2) K. L. Murty, "Beneficial(!) effect of neutron irradiation on mechanical properties of mild steel in blue brittle range," *Scripta Metall.*, **18**[1], 87-89 (1984).
- 3) W. J. Phytiann, A. English, "Microstructural evolution in reactor pressure vessel steels," *J. Nucl. Mater.*, **205**, 162-177 (1993).
- 4) J. T. Buswell, W. J. Phytiann, R. J. McEloy, S. Dumbil, P. H. N. Rayand, J. Mace, R. N. Sinclair, "Irradiation-induced microstructural changes, and hardening mechanisms, in model PWR reactor pressure vessel steels," *J. Nucl. Mater.*, **225**, 196-214 (1995).
- 5) Q. Xu, T. Yoshiie, K. Sato, "Dose dependence of Cu precipitate formation in Fe-Cu model alloys irradiated with fission neutrons," *Phys. Rev.*, **B73**[13], 134115 (2006).
- 6) T. Toyama, Y. Nagai, Z. Tang, M. Hasegawa, A. Almazouzi, E. van Walle, R. Garard, "Nanostructural evolution in surveillance test specimens of a commercial nuclear reactor pressure vessel studied by three-dimensional atom probe and positron annihilation," *Acta Mater.*, **55**[20], 6852-6860 (2007).
- 7) N. Soneda, K. Doi, A. Nomoto, K. Nishida, S. Ishino, *Development of neutron irradiation embrittlement correlation of reactor pressure vessel materials of light water reactor*, CRIEPI Research Report Q06019, Central Research Institute of Electronic Power Industry (CRIEPI) (2006), [in Japanese].
- 8) K. Doi, K. Nishida, A. Nomoto, N. Soneda, H. Watanabe, *3D atom probe observation of heavy ion irradiated model alloys for reactor pressure vessel steels*, CRIEPI Research Report Q08026, Central Research Institute of Electronic Power Industry (CRIEPI) (2009), [in Japanese].
- 9) K. Doi, K. Nishida, A. Nomoto, T. Hamaoka, N. Soneda, *Effect of irradiation temperature on hardening and microstructural changes of heavy ion irradiated reactor pressure vessel model alloys*, CRIEPI Research Report Q09026, Central Research Institute of Electronic Power Industry (CRIEPI) (2010), [in Japanese].
- 10) T. Tsuru, C. Suzuki, Y. Kaji, T. Tsukada, "Non-empirical prediction of impurity segregation in alpha-Fe from first principles," *J. Appl. Phys.*, **107**[6], 061805 (2010).
- 11) T. Ohmura, N. Soneda, M. Iwasawa, "First-principles calculations of vacancy-solute element interactions in body centered cubic iron," *Acta Mater.*, **57**[20], 5947-5955 (2009).
- 12) The "PHASE" code was created by the members of the national project "Frontier Simulation Software for Industrial Science (FSIS)". PHASE ver. 7.01 is downloaded from RSS21 (<http://www.ciss.iis.u-tokyo.ac.jp/rss21/index.html>).
- 13) J. P. Perdew, K. Burke, M. Emzerhof, "Generalized Gradient Approximation Made Simple," *Phys. Rev. Lett.*, **77**[18], 3865-3968 (1996).
- 14) D. Vanderbilt, "Soft self-consistent pseudopotentials in a generalized eigenvalue formalism," *Phys. Rev.*, **B41**[11], 7892-7895 (1990).
- 15) K. Laasonen, A. Pasquarrello, R. Car, C. Lee, D. Vanderbilt, "Car-Parrinello molecular dynamics with Vanderbilt ultrasoft pseudopotentials," *Phys. Rev.*, **B47**[16], 10142-10153 (1993).
- 16) Y. Iwasawa (Ed.), *Kagaku Binran Kisohen* vol. 2, 5th ed., Maruzen, Tokyo, 846-847 (2003).